

REPORT DOCUMENTATION PAGE			Form Approved OMB NO. 0704-0188		
<p>The public reporting burden for this collection of information is estimated to average 1 hour per response, including the time for reviewing instructions, searching existing data sources, gathering and maintaining the data needed, and completing and reviewing the collection of information. Send comments regarding this burden estimate or any other aspect of this collection of information, including suggestions for reducing this burden, to Washington Headquarters Services, Directorate for Information Operations and Reports, 1215 Jefferson Davis Highway, Suite 1204, Arlington VA, 22202-4302. Respondents should be aware that notwithstanding any other provision of law, no person shall be subject to any penalty for failing to comply with a collection of information if it does not display a currently valid OMB control number.</p> <p>PLEASE DO NOT RETURN YOUR FORM TO THE ABOVE ADDRESS.</p>					
1. REPORT DATE (DD-MM-YYYY)		2. REPORT TYPE New Reprint		3. DATES COVERED (From - To) -	
4. TITLE AND SUBTITLE Synthesis and characterization of perfluoro quaternary ammonium anion exchange membranes			5a. CONTRACT NUMBER W911NF-10-1-0520		
			5b. GRANT NUMBER		
			5c. PROGRAM ELEMENT NUMBER 611103		
6. AUTHORS Melissa A. Vandiver, James L. Horan, Yuan Yang, Emily T. Tansey, Söenke Seifert, Matthew W. Liberatore, Andrew M. Herring			5d. PROJECT NUMBER		
			5e. TASK NUMBER		
			5f. WORK UNIT NUMBER		
7. PERFORMING ORGANIZATION NAMES AND ADDRESSES Colorado School of Mines Colorado School of Mines 1500 Illinois Street Golden, CO 80401 -				8. PERFORMING ORGANIZATION REPORT NUMBER	
9. SPONSORING/MONITORING AGENCY NAME(S) AND ADDRESS(ES) U.S. Army Research Office P.O. Box 12211 Research Triangle Park, NC 27709-2211				10. SPONSOR/MONITOR'S ACRONYM(S) ARO	
				11. SPONSOR/MONITOR'S REPORT NUMBER(S) 58161-CH-MUR.19	
12. DISTRIBUTION AVAILABILITY STATEMENT Approved for public release; distribution is unlimited.					
13. SUPPLEMENTARY NOTES The views, opinions and/or findings contained in this report are those of the author(s) and should not be construed as an official Department of the Army position, policy or decision, unless so designated by other documentation.					
14. ABSTRACT In this study, new alkaline exchange membranes were prepared from the perfluorinated 3M ionomer with various quaternary ammonium cations attached with sulfonamide linkage. The degree of functionalization varied depending on the cation species, resulting in different ion exchange capacities (IECs), 0.33–0.72 meq g ⁻¹ . There was evidence of polymer degradation when the films were exposed to hydroxide, and hence all membrane characterization was performed in the chloride form. Conductivity was dependent on cation species and IEC, Ea ¼					
15. SUBJECT TERMS ionomers; fluoropolymers; NMR; SAXS					
16. SECURITY CLASSIFICATION OF:			17. LIMITATION OF ABSTRACT UU	15. NUMBER OF PAGES	19a. NAME OF RESPONSIBLE PERSON Andrew Herring
a. REPORT UU	b. ABSTRACT UU	c. THIS PAGE UU			19b. TELEPHONE NUMBER 303-384-2082

Report Title

Synthesis and characterization of perfluoro quaternary ammonium anion exchange membranes

ABSTRACT

In this study, new alkaline exchange membranes were prepared from the perfluorinated 3M ionomer with various quaternary ammonium cations attached with sulfonamide linkage. The degree of functionalization varied depending on the cation species, resulting in different ion exchange capacities (IECs), 0.33–0.72 meq g⁻¹. There was evidence of polymer degradation when the films were exposed to hydroxide, and hence all membrane characterization was performed in the chloride form. Conductivity was dependent on cation species and IEC, E_a ¼ 36–59 kJ mol⁻¹. Diffusion of water through the membrane was relatively high 1.6×10^{-5} cm² s⁻¹ and indicated restriction over a range of diffusion times, 6–700 ms. Water uptake (WU) in the membranes was generally low and the hydration level varied based on cation species, k ¼ 6–11. Small-angle scattering experiments suggested ionic aggregation, 37–42 Å², independent of cation species but slight differences in long-range order with cation species.

REPORT DOCUMENTATION PAGE (SF298)
(Continuation Sheet)

Continuation for Block 13

ARO Report Number 58161.19-CH-MUR

Synthesis and characterization of perfluoro quat ...

Block 13: Supplementary Note

© 2012 . Published in Journal of Polymer Science Part B: Polymer Physics, Vol. Ed. 0 (2012), (Ed.). DoD Components reserve a royalty-free, nonexclusive and irrevocable right to reproduce, publish, or otherwise use the work for Federal purposes, and to authorize others to do so (DODGARS §32.36). The views, opinions and/or findings contained in this report are those of the author(s) and should not be construed as an official Department of the Army position, policy or decision, unless so designated by other documentation.

Approved for public release; distribution is unlimited.

Synthesis and Characterization of Perfluoro Quaternary Ammonium Anion Exchange Membranes

Melissa A. Vandiver,¹ James L. Horan,¹ Yuan Yang,² Emily T. Tansey,¹ Söenke Seifert,³ Matthew W. Liberatore,¹ Andrew M. Herring¹

¹Department of Chemical and Biological Engineering, Colorado School of Mines, Golden, Colorado 80401-1887

²Department of Chemistry and Geochemistry, Colorado School of Mines, Golden, Colorado 80401-1887

³X-Ray Science Division, Argonne National Laboratory, Argonne, Illinois 60439

Correspondence to: A. M. Herring (E-mail: aherring@mines.edu)

Received 22 June 2012; revised 15 August 2012; accepted 27 August 2012; published online

DOI: 10.1002/polb.23171

ABSTRACT: In this study, new alkaline exchange membranes were prepared from the perfluorinated 3M ionomer with various quaternary ammonium cations attached with sulfonamide linkage. The degree of functionalization varied depending on the cation species, resulting in different ion exchange capacities (IECs), 0.33–0.72 meq g⁻¹. There was evidence of polymer degradation when the films were exposed to hydroxide, and hence all membrane characterization was performed in the chloride form. Conductivity was dependent on cation species and IEC, $E_a = 36$ –59 kJ mol⁻¹. Diffusion of water through the membrane

was relatively high 1.6×10^{-5} cm² s⁻¹ and indicated restriction over a range of diffusion times, 6–700 ms. Water uptake (WU) in the membranes was generally low and the hydration level varied based on cation species, $\lambda = 6$ –11. Small-angle scattering experiments suggested ionic aggregation, 37–42 Å, independent of cation species but slight differences in long-range order with cation species. © 2012 Wiley Periodicals, Inc. *J Polym Sci Part B: Polym Phys* 000: 000–000, 2012

KEYWORDS: ionomers; fluoropolymers; NMR; SAXS

INTRODUCTION The proton exchange membrane (PEM) fuel cell is a very attractive energy conversion device owing to its high power density; however, it suffers from a number of disadvantages including the requirement for precious metal catalysts and the challenge of oxidizing complex fuels under acidic conditions.^{1–3} Recently, there has been increasing interest in using alkaline fuel cells (AFCs) owing to the potential to utilize less expensive metal catalysts and the ability to oxidize more complex fuels such as ethanol.^{2,4–6} Traditional AFCs utilize a liquid electrolyte of aqueous potassium hydroxide; however, exposure to carbon dioxide generates insoluble potassium carbonate/bicarbonate precipitates that can block active sites on the electrodes reducing performance.^{2,4,6,7} Recent research on alkali fuel cells has focused on the development of a solid anion exchange membrane (AEM) electrolyte that would combine the engineering benefit of a solid polymer electrolyte and kinetic advantages of an alkali fuel cell. The role of water in ion conduction and AEM stability needs to be understood for practical commercialization of an AEM fuel cell. Although adequate hydroxyl conductivity has been demonstrated in AEMs under very wet conditions,^{8–10} conductivity rapidly diminishes at lower relative humidity (RH), and the stability of the cations in the polymers may be an issue for long-term operation.^{2,4,6} It is, therefore, important that anion conductivity in AEMs be

understood in detail with respect to polymer morphology, water content, and cation chemistry.

Perfluorosulfonic acid (PFSA) membranes have dominated the PEM fuel cell industry owing to their high proton conductivity, and sufficient chemical and mechanical stability.^{5,11} Du Pont introduced their PFSA membrane, NafionTM, in the 1970s which exhibited higher conductivity and a longer lifetime compared to earlier PEMs.¹ Today, Nafion and other PFSA membranes remain the industry standard for PEMs and the benchmark to which all new PEMs and AEMs are compared.^{1,12} The performance and stability of PFSA, along with the vast literature available for comparison,¹³ has generated interest in synthesis of a perfluorinated AEM based on the same polymer architecture. There have been several studies on perfluorinated AEMs synthesized by the functionalization of a PFSA precursor with a cationic species.^{14–17} The reported conductivity and cation stability varied greatly for these membranes, indicating further study is necessary to evaluate the potential for perfluorinated AEMs.

Chemical stability is a fundamental requirement for an AEM; however, most common cation species used in AEMs exhibit some level of degradation in hydroxide.² Common cation groups used in AEMs include quaternary ammonium, quaternary phosphonium-, tertiary sulfonium-, and guanidinium-based

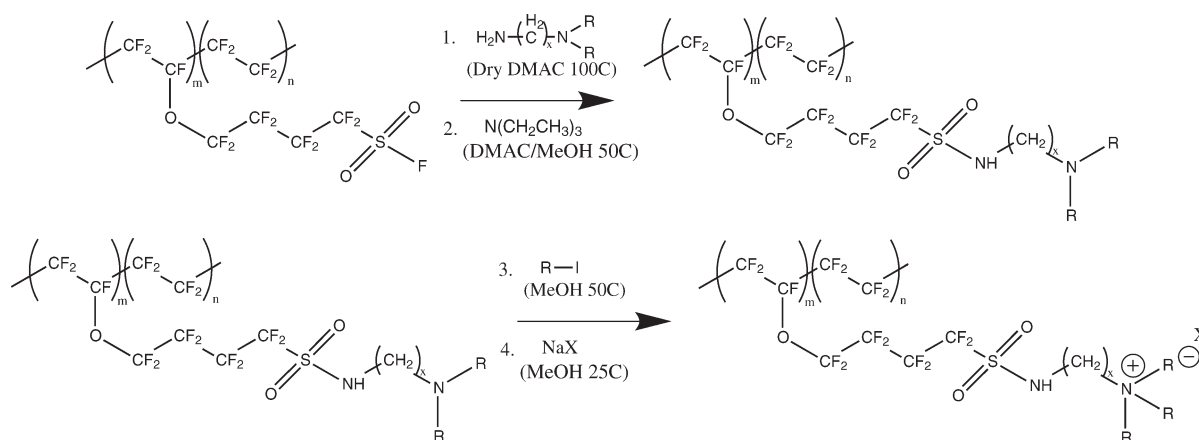


FIGURE 1 Reaction scheme for the functionalization of the 3M sulfonfyl fluoride ionomer with quaternary ammonium cations.

compounds.⁴ Unfortunately, degradation is a concern for all of these cations, making production of a stable AEM difficult. The most widely used cations for AEMs are quaternary ammonium compounds, which suffer a number of hydroxide degradation routes. Quaternary ammonium compounds can undergo Hoffman elimination to form an amine and an olefin, nucleophilic substitution to produce an amine and an alcohol, and elimination of hydrogen to form water and an ylide, which further reacts to form an amine and an olefin.^{2,4,18} Some of these degradation pathways can be avoided or reduced by careful selection of cation species.² Degradation of quaternary ammonium cations by hydroxide has been studied for cations in solution,^{18,19} but the stabilities of these cations tethered to a polymer have not been fully characterized. Direct comparison of cation species effects on membrane conductivity, morphology, and stability is necessary as AEM development progresses toward practical application.

In this study, we have functionalized a commercially produced perfluorinated ionomer with three different quaternary ammonium cation species to produce perfluoroquaternary ammonium (PFQA) AEMs. The three cation species reacted to different degrees, resulting in a range of ion exchange capacities (IECs). These polymer membranes were evaluated as potential AEMs based on conductivity, water diffusion, WU, and polymer morphology. Membrane conductivity, WU, and morphology all varied, to some degree, based on the cation species tethered to the polymer with the smallest methyl ammonium cation having the highest conductivity and WU. Unfortunately, all of these membranes displayed significant degradation by hydroxide and further study would be needed to produce stable cation species on a perfluorinated AEM.

EXPERIMENTAL

Materials

The sulfonfyl fluoride version of the perfluorinated ionomer at 800 EW was supplied in powder form by 3M. All other chemicals were purchased from Sigma Aldrich and were of reagent grade.

Synthesis and Processing

The reaction scheme to synthesize the PFQA polymer was based on the patent by Matsui,²⁰ with modifications to the solvent to increase polymer swelling, extension of reaction times to improve conversion, and an additional washing step with triethylamine to remove an acid by-product that would have hindered the alkylation step. In a typical synthesis, the dried (vacuum oven, overnight, 50 °C) 3M ionomer (10 g) was first swelled in anhydrous dimethylacetamide, about 25 cm³, decanted from molecular sieves, at a temperature of 100 °C. The perfluorosulfonyl material was aminated using a 10-fold molecular excess of the diamine, consisting of a 3-carbon methylene chain with a primary amine on one end and a tertiary amine on the other, such as 3-(dimethylamino)-1-propylamine. The solvent was then removed and treated with triethylamine (15 cm³) to completely remove the HF byproduct and the product again dried by rotovap. A 10-fold excess of alkyl iodide was then introduced to the reaction vessel to quaternize the terminal amine. The material was then dried and treated with a fivefold excess LiCl in MeOH (25 cm³) overnight, followed by solvent removal and drying in a vacuum oven. The final product was separated from the excess LiCl by thoroughly washing with water, and a final drying step to give a light brown powder. After quaternization, the counter-ion associated with the cation can be changed by an ion exchange reaction. The ion exchange reaction involves soaking the material in a 1 M solution of the desired ion solution for at least 24 h. Following the ion exchange reaction, the material must be washed thoroughly with water to remove excess ions from the polymer. The overall reaction scheme followed is shown in Figures 1 and 2, indicating the functionalized cation structures of the resulting materials. The polymers were cast into membranes from dimethylacetamide on Teflon blocks and dried under reduced pressure (200 mbar) at 70 °C, to give light brown brittle films, 70–150 μm.

Measurements

Fourier transform infrared (FTIR) spectra were obtained on a Nicolet Nexux 470 FTIR ESP with an attached Specac

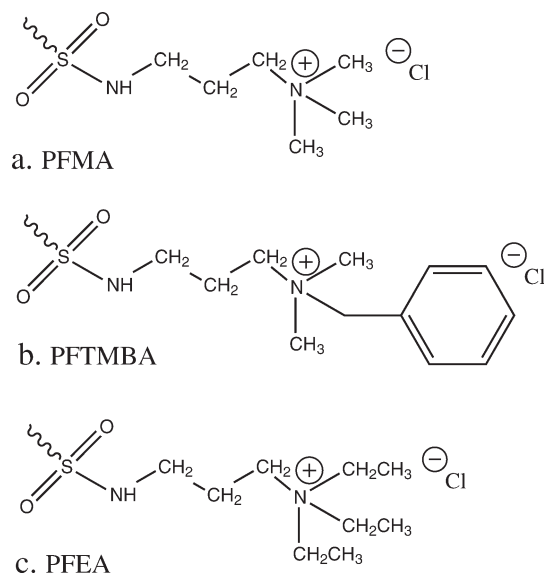


FIGURE 2 Resulting cation structures after functionalization of the sulfonyl group, the curved bond represents the sulfur attachment to the pendant chain of polymer. The resulting species are (a) methyl ammonium (PFMA), (b) trimethylbenzyl ammonium (PFTMBA), and (c) ethyl ammonium (PFEA).

Diamond attenuated total reflectance (ATR) attachment. Typical spectrum range was 4000–500 cm^{-1} with a resolution of 4 cm^{-1} and 128 scans. The ^1H NMR spectrum was obtained using a Jeol ECA-500 Spectrometer at 500 MHz. Analysis of the spectra was performed using the Delta spectral software.

The IEC of the material was determined by titrating the chloride ions in solution after soaking chloride-form membranes in 1 M sodium bicarbonate solutions for 48 h. Standardized silver nitrate solution was used to titrate the membrane solutions with a potassium chromate indicator. The end point for the titration was defined as the point where permanent rust-colored precipitates were observed in solution.

The in-plane conductivities of the membranes were calculated using electrochemical impedance spectroscopy to measure membrane resistance as given by eq 1.

$$\sigma = \frac{l}{R \cdot w \cdot t} \quad (1)$$

where R is the membrane resistance, l is the distance between the electrodes, w is the width of the membrane samples, and t is the thickness of the sample. Impedance spectra were obtained over a frequency range of 1–10⁵ Hz using a four-electrode test cell connected to a BioLogic VMP3 multichannel Potentiostat. The measurements were made in a TestEquity environmental chamber to control sample temperature and humidity. The resistance of the membrane was determined from the low-frequency intercept of the Nyquist impedance plot. All samples were in the chloride form and experiments were performed at constant RH of 80 or 95%, varying temperature from 50 to 90 °C in 10 °C steps.

Self-diffusion coefficients were measured by pulsed-field gradient nuclear magnetic resonance (PFG-NMR) spectroscopy with a stimulated echo pulse sequence. Pulse gradient NMR experimental data were analyzed by using the Stejskal-Tanner equation^{21,22} given in eq 2

$$\frac{S}{S_0} = e^{-\gamma^2 G^2 \delta^2 (\Delta - \frac{\delta}{3}) D} \quad (2)$$

where S and S_0 represent the signal amplitude and the signal amplitude at zero gradient, γ is the gyro magnetic ratio, G is the gradient strength, δ is the gradient pulse length, Δ is the diffusion time, and D is the apparent diffusion coefficient. Membrane samples were wound into a cylinder and suspended above saturated salt solution in a 5-mm NMR tube to generate an environment of 80% RH. A pulse gradient-stimulated echo sequence was performed using a Bruker AVANCEIII NMR spectrometer and 400 MHz wide bore Magnetex Magnet. Proton diffusion measurements were made using a 5-mm Bruker single-axis DIF60L Z-diffusion probe. The 90° pulse length was on the order of 5.0 μs . Typical parameters at 25 °C were $G = 0$ –128 G cm^{-1} , incremented in 16 steps, $\delta = 1$ ms, $\Delta = 6$ –700 ms. The Bruker TopSpin software was used for data acquisition and analysis. Multiple diffusion experiments were performed varying the time between pulses, (Δ), between 6 and 700 ms with a constant gyromagnetic ratio (γ) of 4258 Hz G^{-1} and pulse length (δ) of 1 ms. The maximum gradient strength for each experiment was chosen to produce a full decay of the signal intensity over the length of the experiment. The decay of the signal intensity was plotted against gradient strength for each experiment and fit to eq 2 to determine the diffusion coefficient.

WU was characterized using a SMS dynamic vapor sorption apparatus. A small-membrane sample, about 25 mm^2 , was placed on a glass weigh plate and change in mass was measured gravimetrically under different humidity conditions. Humidity was cycled between dry and saturated conditions in steps of 20% RH. The WU of the membrane was calculated based on eq 3

$$\text{WU} = \frac{m_{\% \text{RH}} - m_{\text{dry}}}{m_{\text{dry}}} \times 100 \quad (3)$$

where $m_{\% \text{RH}}$ is the mass of the sample at the given RH and m_{dry} is the mass of the dry sample. Given the WU at saturated conditions and the known IEC of the membrane the hydration level, λ , which is the number of waters per cation functional group can be calculated using eq 4

$$\lambda = \frac{n(\text{H}_2\text{O})}{n(\text{NR}_4^+)} = \frac{\text{WU}}{m(\text{H}_2\text{O}) \cdot \text{IEC}} \quad (4)$$

where $m(\text{H}_2\text{O})$ is the molar mass of water. The mass of the membrane was monitored as a function of time while incrementally changing the RH. The mass of the dry membrane was taken as the measured mass at the end of the initial 4-h drying period. The WU was calculated based on eq 3 using

the measured mass at the steady state of each 2-h humidity step.

Small angle X-ray scattering experiments were performed at The Basic Energy Sciences Synchrotron Radiation Center, beamline 12-ID-B, at the Advanced Photon Source at Argonne National Lab. Measurements were taken in a transmission geometry using a Pliatus 2M SAXS detector and a Pliatus 300K WAXS detector with an acquisition time of 1 s at a beam energy of 12 keV and incoming X-ray wavelength of 1 Å. The 2D scatter was radially integrated to obtain data of intensity versus scattering vector q . The transmission intensity was normalized to exposure time and flux of the direct beam through the sample. However, because of the swelling of the samples tested, absolute thickness and atomic density could not be determined *in situ* and the intensity units become arbitrary. A custom-built four-sample oven controlled the humidity and temperature of the samples during scattering experiments. Typical experiments contained three membrane samples and one empty window and hence a background spectrum could be obtained throughout the scattering experiment. The humidity of sample environment was controlled using a combination of wet and dry nitrogen. Samples were removed from water, blotted dry, and mounted on the sample holders using KaptonTM tape. Samples were inserted into the oven maintained at 60 °C and 95% RH. The samples were allowed to take up water for 20 min before X-ray spectra were taken. Humidity was then stepped down to 75, 50, 25%, and dry gas in 15-min steps. After the dry step was completed, the humidity was set directly to 95% RH for 15 min to test for hysteresis of the membranes.

RESULTS AND DISCUSSION

The synthesis of the polymer followed the reaction scheme in Figure 1 to produce the three polymers shown in Figure 2. Characterization of the progress of the reaction and final reaction product were performed using a combination of FTIR, NMR, and chloride titration. FTIR spectra were obtained for the precursor material and following the amination and quaternization reactions (Fig. 3). All of the aminated materials displayed new peaks, indicating attachment of the amine to the polymer. Following the quaternization reaction, all of the materials showed a broad peak at 3500 cm^{-1} . The 3M-sulfonyl precursor material showed broad absorbance peaks between 1300 and 1100 cm^{-1} corresponding to the C—F bonds along the backbone and side chain. All spectra were normalized to the high intensity peak at 1200 cm^{-1} owing to the stability of the C—F backbone throughout the reaction. The precursor material also showed a distinct peak at 1470 cm^{-1} that is associated with S—F motion²³ or the asymmetric stretch of the SO_2F group.¹⁶ This peak is drastically reduced upon amination where the S—F bond is replaced by an S—N bond. The S—N bond produces a new peak at 1375 cm^{-1} .²⁴ The peak at 1470 cm^{-1} was not reduced completely, suggesting incomplete reaction of the sulfonyl groups. The unreacted sulfonyl groups can hydrolyze to sulfonic acid upon exposure to water, which would produce distinct new peaks at 1290 and 1060 cm^{-1} .²⁵ However,

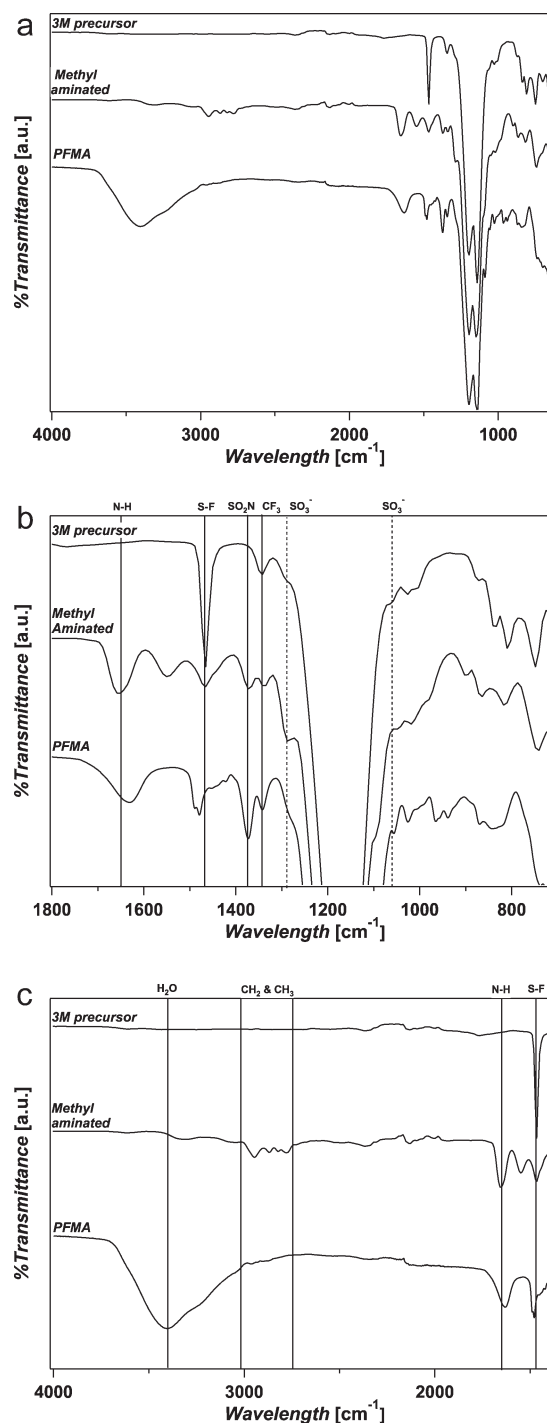


FIGURE 3 (a) Full IR spectra of the 3M sulfonyl precursor, methyl aminated polymer, and quaternized methyl ammonium polymer. (b) Magnification of the spectra to highlight the reduction of the S—F peak at 1470 cm^{-1} , addition of the SO_2N peak at 1375 cm^{-1} and N—H peak at 1650 cm^{-1} , and the lack of distinct sulfonic acid peaks at 1290 and 1060 cm^{-1} . (c) Magnification of the spectra to highlight the CH_2 and CH_3 peaks between 3000 and 2700 cm^{-1} and the broad peak between 3600 and 3000 cm^{-1} owing to water association with the cation group.

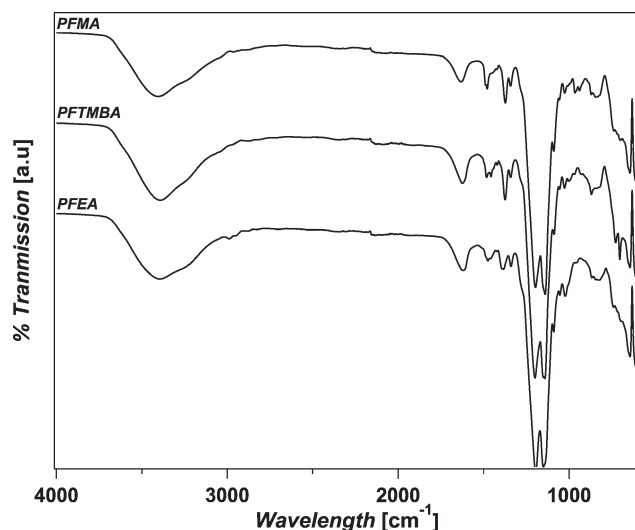


FIGURE 4 IR spectra of all PFQA polymers following the quaternization reaction step. The PFMA, PFTMBA, and PFEA all show a broad peak at 3500 cm^{-1} owing to the coordination of water to the ammonium as well as the alkyl peaks from the amine.

the regions at 1290 and 1060 cm^{-1} display only low-absorbance shoulders similar to the precursor spectra, suggesting conversion to sulfonic acid was very minor. The attachment of the diamine to the sulfonyl produces new peaks at 1650 cm^{-1} corresponding to the N—H bond and 3000 and 2700 cm^{-1} corresponding to the C—H bonds of the alkyl groups of the diamine. Figure 4 shows the spectra of all perfluorinated polymers following the quaternization reaction step. A broad peak between 3600 and 3000 cm^{-1} is present after the alkylation reaction owing to the O—H bond of water coordinating with the newly formed quaternary ammonium cation group. There is little difference between the FTIR of the quaternized polymers owing to their similar chemical compositions.

^1H NMR experiments were performed on the methyl and trimethylbenzyl ammonium samples to confirm the chemical attachment and structure of the quaternized polymer species. The ethyl ammonium polymer did not adequately dissolve in any common NMR solvents preventing ^1H NMR characterization. All materials were thoroughly washed to remove residual salts following the LiCl ion exchange treatment and dried overnight in a vacuum oven before NMR sample preparation. The ^1H NMR spectra for the methyl and trimethylbenzyl ammonium polymers showed peaks representing the alkyl chain of the amine and quaternary ammonium groups; however, the spectra had additional peaks that were not easily identified. In the ^1H NMR (Fig. 5) the methylene protons are assigned to the protons at 1.1, 2.15, and 2.4 ppm and the methyl of the quaternary ammonium at 2.6 ppm. The proton on the sulfonamide is tentatively assigned to the shoulder at 3.0 ppm. Three additional peaks marked with asterisk in the figure were observed. From separate experiments, it was shown that the reaction of the diamine

with alkyl iodide produced a white salt that was insoluble in water and common organic solvents. Tentatively, we assign these peaks to the fully quaternized diamine, which would now be symmetrical giving rise to methylene peaks at 0.2 and 1.0 ppm and the methyls of the quaternary ammonium at 2.5 ppm. It is suspected that excess diamine was preserved in the polymer and quaternized during alkylation or that the diamine detached during the quaternization reaction and was further alkylated, producing the insoluble salt that is responsible for the additional proton peaks in the ^1H NMR spectra. Further evidence for this was shown in the ^1H NMR of the trimethylbenzyl polymer where the dication coproduct is now not symmetrical, resulting in a complex ^1H NMR spectrum (data not shown).

One objective of this study was to study the anionic transport of this material in the hydroxide form. However, several experiments clearly proved that the cationic linkage chemistry was not sufficiently stable for this characterization. In a standard acid/base titration to determine membrane IEC, in which the membranes were treated with sodium hydroxide in the first step, the calculated IECs were exceedingly low, three orders of magnitude lower than when a chloride ion titration was performed (see below). The extremely low IEC values calculated from the acid/base titration suggested that the membranes were not stable in hydroxide solution and resulted in the loss of cation groups. An attempt was also made to measure the ionic conductivity of the PFQA membrane in the hydroxide form using a modified BekkTech cell that allowed *in situ* hydroxide exchange, followed by thorough washing, and measurement with rigorous exclusion of carbon dioxide. During this test, the membrane conductivity steadily decreased with time, again suggesting chemical degradation by hydroxide. Membranes exposed to hydroxide and later exchanged back to the chloride form produced much

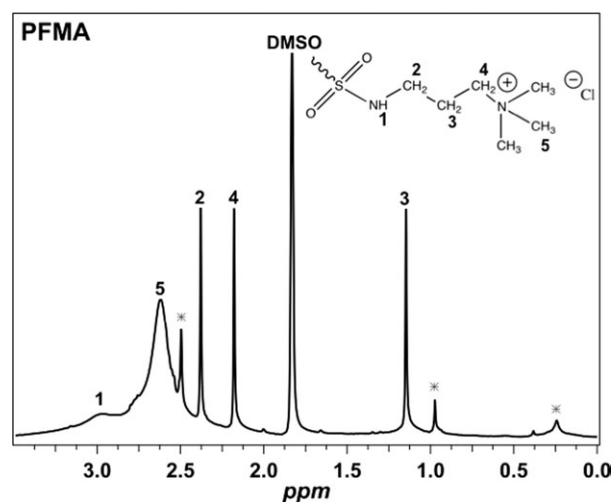


FIGURE 5 ^1H NMR spectra of the PFMA polymer. The peaks identified as the alkyl and ammonium hydrogens are shown on corresponding chemical structure. Unidentified peaks, thought to be a result of insoluble diamine salts, are labeled with a star.

TABLE 1 Summary of the IEC, Conductivity, and Corresponding Activation Energy, WU, and Diffusion Coefficient for PFQA Polymer Membranes^a

Material	IEC (meq g ⁻¹)	σ (mS cm ⁻¹)	E_a (kJ mol ⁻¹)	WU (%)	λ	D (cm ² s ⁻¹)
PFMA	0.72 ± 0.02	4.8 ± 0.1	36 ± 5	8.0 ± 0.2	6.2 ± 0.2	1.6 × 10 ⁻⁵
PFTMBA	0.52 ± 0.02	3.3 ± 0.2	59 ± 5	7.1 ± 0.1	7.6 ± 0.3	–
PFEA	0.33 ± 0.01	0.6 ± 0.5	50 ± 14	6.6 ± 0.1	11.0 ± 0.4	–

^a The conductivity and WU are for saturated conditions at 60 °C. The diffusion coefficient was measured at 80% RH and 25 °C.

lower conductivities than pristine membrane samples, confirming that hydroxide irreversibly altered membrane chemistry. There is evidence in literature that ammonium¹⁷ and guanidium²⁶ cations attached directly to the side chain of a perfluorinated polymer are unstable in hydroxide. To understand the relationship of anion conductivity to cation size and polymer morphology, all characterization and testing were performed on the polymers in the chloride form to ensure that the data were not biased by the instability of the polymer in the hydroxide form.

The extent of quaternization, reflected by the IEC (Table 1) had a significant effect on polymer performance as will be shown in the characterization of the materials. The methyl

ammonium material quaternized to the fullest extent giving it the highest IEC, 0.72 meq g⁻¹, the maximum theoretical IEC being about 1.0 meq g⁻¹. The trimethylbenzyl ammonium and ethyl ammonium materials had IEC values of 0.52 and 0.33 meq g⁻¹, respectively. The lower IECs of the larger cations were a result of the steric hindrance of the larger alkyl groups on the amine and larger alkylating group that restricted quaternization of the amine.

Ionic conductivity of the quaternized species was performed using electrochemical impedance spectroscopy at temperatures of 50–90 °C and constant RH. This experimental method allowed calculation of the energy of activation (E_a) for ion conduction in the material by an Arrhenius relationship (Table 1). Figure 6 shows the conductivity for all polymer samples at 80 and 95% RH. The conductivity increased for all polymer samples with increased temperature and humidity. The conductivity was highest for the methyl ammonium polymer, followed by the trimethylbenzyl and ethyl ammonium. Conductivity increased with increasing IEC at both humidities (Fig. 7). The activation energies calculated for the PFQA materials ranged from 36–59 kJ mol⁻¹ (Table 1). These activation energies are very high compared to the reported activation energies for NafionTM that range from 5 to 20 kJ mol⁻¹^{127,28} and those for other AEM (10–25 kJ mol⁻¹).^{9,28} The high activation energies for the PFQA membranes, even at high humidities, may suggest the percolation networks generated in hydrated PFSA^{13,29,30} membranes do not extend fully for the AEMs tested.

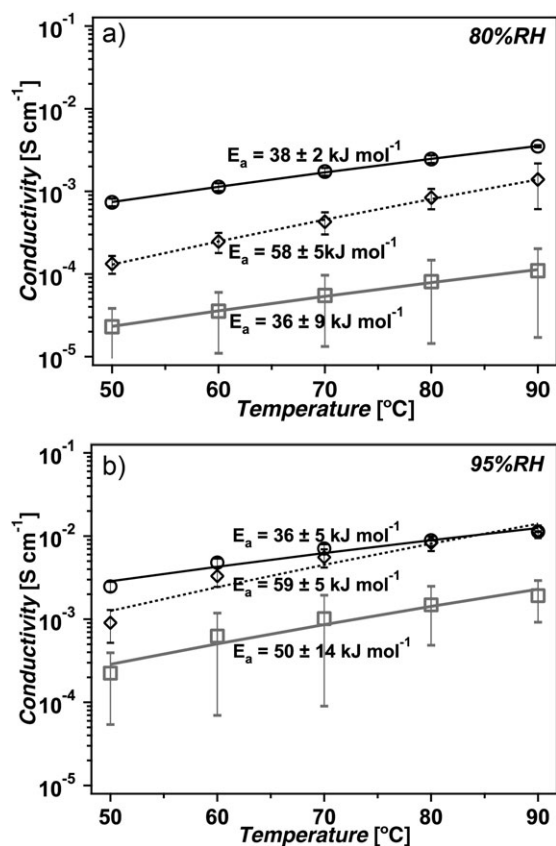


FIGURE 6 Conductivity of PFMA ○, PFTMBA ◆, PFEA ■ at (a) 80% RH and (b) 95% RH versus temperature. The markers represent the experimental data and the lines represent the Arrhenius fit used to calculate activation energy.

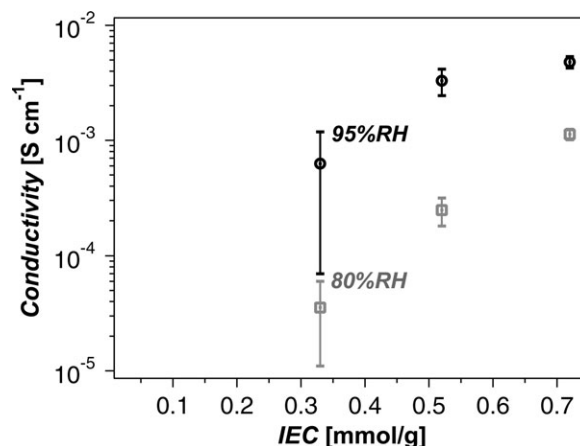


FIGURE 7 Conductivity as a function of IEC, all measurements are at 60 °C, the data sets are for 80% RH and 95% RH.

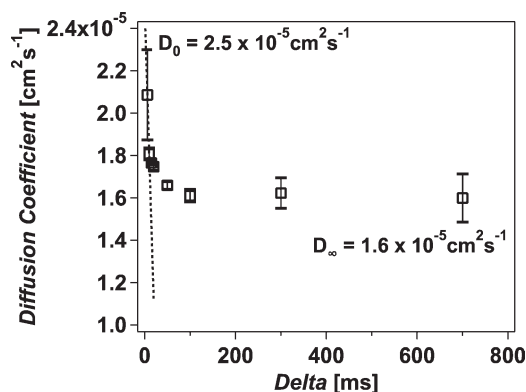


FIGURE 8 Calculated self-diffusion coefficient of water through the methyl ammonium membrane at different Δ values, the time between the gradient pulses.

PFG-NMR was performed on the methyl ammonium polymer to determine the diffusion of water through the membrane. The calculated diffusion coefficient was plotted versus the time between gradient pulses (Δ) to evaluate the restriction of diffusion in the membrane along different length scales (Fig. 8). The calculated diffusion coefficient decreased as the time between gradient pulses was increased, indicating restriction to diffusion in the membrane. By regression of the diffusion coefficient to a Δ of zero the free diffusion coefficient D_0 was determined to be $2.5 \times 10^{-5} \text{ cm}^2 \text{ s}^{-1}$ which is slightly larger than the free diffusion coefficient of liquid water,^{31,32} suggesting that these data overestimate the free diffusion coefficient of water in the membrane. The bulk, or infinite, diffusion coefficient is taken as the diffusion coefficient at the largest Δ and was equal to $1.6 \times 10^{-5} \text{ cm}^2 \text{ s}^{-1}$. These values are relatively high compared to diffusion coefficients reported for NafionTM which are generally $<1 \times 10^{-5} \text{ cm}^2 \text{ s}^{-1}$.^{33–36} The high diffusion through the membrane may indicate a different long range ordering in the quaternary ammonium membranes compared to PFSA membranes. The relatively low ionic conductivity observed in the PFQA membranes compared to the high diffusion suggests that the ionic transport mechanism is different from the water transport mechanism for the membrane in the chloride form.

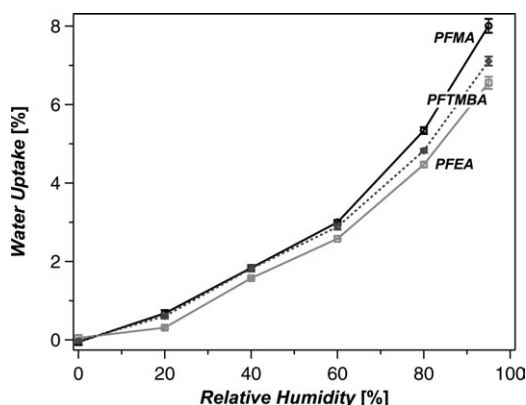


FIGURE 9 WU for PFQA membranes at relative humidities between 0 and 95% RH, lines are just for clarity.

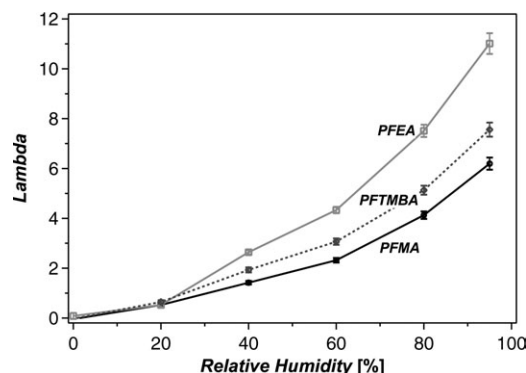


FIGURE 10 Hydration level of the PFQA membranes at relative humidities from 0 to 95% RH, lines are just for clarity.

WU in the membrane was measured gravimetrically in a dynamic vapor sorption apparatus (Fig. 9). WU was greatest for the methyl ammonium material with a maximum WU of about 8 wt %, followed closely the trimethylbenzyl and ethyl ammonium polymers. This level of WU is significantly lower than that of PFSA membranes. The trend of WU values corresponds with the IECs and performance of the membranes in conductivity experiments; however, the difference in WUs is less than expected, given the significant difference in IECs. The hydration level (Fig. 10) has a reverse trend from the WU measurements. The ethyl ammonium material showed the largest number of coordinating waters, $\lambda = 11$ at 95% RH, followed by the trimethylbenzyl and methyl ammonium materials, $\lambda = 8$ and 6, respectively. The similar WU but different hydration levels based on cation suggests that the solvation structures of the cations are different.

Morphology and membrane swelling were characterized using small angle X-ray scattering. The dominant feature of the SAXS spectra for the PFQA materials is a peak around 0.15 \AA^{-1} (Fig. 11). This feature is similar to the “ionomer peak” of PFSA materials that corresponds to the ionic aggregates of the polymer where water will be contained for swollen membranes.^{29,30,37} This peak in the PFQA materials is larger for the dry membranes about 40 \AA , compared to PFSA materials about 30 \AA .^{38,39} The peak shifts to lower q as the humidity is increased owing to the expansion of the ionic domain with water. Membrane swelling of the ionic region did not depend on cation species with all membranes having a 4–5 \AA increase of the ionic region from a dry to humidified state (Fig. 12). The increase in size of the ionic region in the PFQAs is low compared to PFSA, which generally have a 10–15 \AA increase in size from a dry to humidified state.^{38,39} The lower swelling of the PFQA membrane is expected, given the low WU of these membranes. Although all the samples showed a slight shift in peak position, the shape and features of this region remained constant, indicating no major structural reorganization of the ionic aggregates; this could contribute to the low ionic conductivity of the PFQA membranes. The position of the SAXS spectra upturn between 0.03 and 0.04 \AA^{-1} differed with

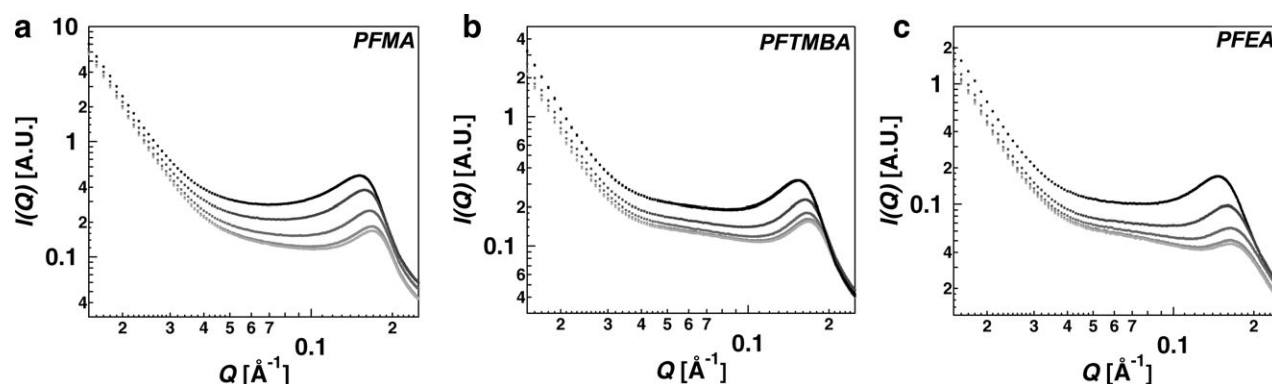


FIGURE 11 SAXS spectra for the PFQA membranes (a) PFMA, (b) PFTMBA, (c) PFEA, the black data represent the humidified membranes at 95% RH with the colors getting lighter as humidity is decreased to 75, 50, and 25% and finally 0% RH as the lightest gray data.

respect to the functionalized cation species and suggested different long polymer orderings in the membranes with cation species [Fig. 12].

CONCLUSIONS

In this study, a perfluorinated polymer was functionalized with different quaternary ammonium cation species and the resultant PFQAs evaluated as potential AEMs. Acid–base titration and conductivity in the hydroxide form indicated all polymers suffered chemical degradation by hydroxide, eliminating the cation species from the polymer. Although reaction conditions were maintained constant for all polymers, the degree of functionalization varied with cation species, resulting in different IECs. Larger cation species had lower degrees of quaternization owing to steric hindrance during the alkylation reaction, highlighting the need to consider cation species and synthetic route during AEM development. Conductivity was shown to be highly dependent on cation species and IEC, and the activation energy for ion conduction was relatively high compared to PFSA and other AEMs. The smallest cation species, methyl ammonium, reacted to the fullest and had the highest conductivity and hence it was the focus of additional

study. Diffusion of water through the methyl ammonium membrane showed restriction over different diffusion times. Overall, the fast diffusion of water in the membrane may indicate that the water transport mechanism is different than the ionic conduction mechanism for the PFQA systems in the chloride form. WU was generally low for the PFQA materials and hydration level varied based on cation species, suggesting different solvation structures. Small-angle scattering experiments suggested ionic aggregation in PFQA materials similar to PFSA membranes that did not depend on the cation species, but other SAXS features suggested slight differences in long-range order with cation species. The significant differences in membrane conductivity, WU, and morphology based on functionalized cation species highlight the importance of considering cation species when developing an AEM. The PFQA membranes suffered from significant degradation from hydroxide signifying the need for the development of more stable cation species and chemical linkage to the polymer before a perfluorinated AEM could be commercialized. Future study will focus on developing a different chemical attachment of the cation to the sulfonyl group and different cation species to improve polymer stability.

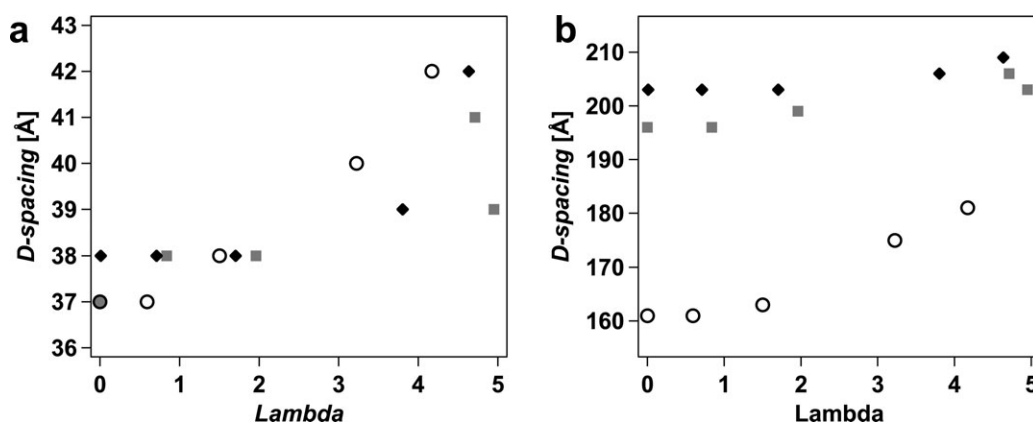


FIGURE 12 D-spacing of the (a) ionomer peak and (b) SAXS upturn with respect to the hydration level of the membranes at the different humidities evaluated during the SAXS experiments. PFMA ○, PFTMBA ◆, and PFEA ■.

ACKNOWLEDGMENTS

The authors thank the Army Research Laboratory for support of this research under the MURI grant number #W911NF-10-1-0520. The authors thank Steven J. Hamrock of 3M Company for useful discussions and supplying the 3M ionomer. Use of the Advanced Photon Source, an Office of Science User Facility operated for the U.S. Department of Energy (DOE) Office of Science by Argonne National Laboratory, was supported by the U.S. DOE under Contract No. DE-AC02-06CH11357.

REFERENCES AND NOTES

- 1 Smitha, B.; Sridhar, S.; Khan, A. A. *J. Membr. Sci.* **2005**, *259*, 10–26.
- 2 Varcoe, J. R.; Slade, R. C. T. *Fuel Cells* **2005**, *5*, 187–200.
- 3 DeLuca, N. W.; Elabd, Y. A. *J. Polym. Sci. Part A: Polym. Phys.* **2006**, *44*, 2201–2225.
- 4 Couture, G.; Alaaeddine, A.; Boschet, F.; Ameduri, B. *Prog. Polym. Sci.* **2011**, *36*, 1521–1557.
- 5 Di Noto, V.; Zawodzinski, T. A.; Herring, A. M.; Giffin, G. A.; Negro, E.; Lavina, S. *Int. J. Hydrogen Energy* **2012**, *37*, 6120–6131.
- 6 Merle, G. R.; Wessling, M.; Nijmeijer, K. J. *J. Membr. Sci.* **2011**, *377*, 1–35.
- 7 McLean, G. F.; Niet, T.; Prince-Richard, S.; Djilali, N. *Int. J. Hydrogen Energy* **2002**, *27*, 507–526.
- 8 Varcoe, J. R.; Slade, R. C. T.; Lam How Yee, E.; Poynton, S. D.; Driscoll, D. J.; Apperley, D. C. *Chem. Mater.* **2007**, *19*, 2686–2693.
- 9 Yan, J.; Hickner, M. A. *Macromolecules* **2010**, *43*, 2349–2356.
- 10 Hibbs, M. R.; Fujimoto, C. H.; Cornelius, C. J. *Macromolecules* **2009**, *42*, 8316–8321.
- 11 Neburchilov, V.; Martin, J.; Wang, H.; Zhang, J. *J. Power Sources* **2007**, *169*, 221–238.
- 12 Hickner, M. A.; Ghassemi, H.; Kim, Y. S.; Einsla, B. R.; McGrath, J. E. *Chem. Rev.* **2004**, *104*, 4587–4612.
- 13 Mauritz, K. A.; Moore, R. B. *Chem. Rev.* **2004**, *104*, 4535–4586.
- 14 Kong, X.; Wadhwa, K.; Verkade, J. G.; Schmidt-Rohr, K. *Macromolecules* **2009**, *42*, 1659–1664.
- 15 Jung, M.-S. J.; Arges, C. G.; Ramani, V. *J. Mater. Chem.* **2011**, *21*, 6158–6160.
- 16 Salerno, H. L. S.; Beyer, F. L.; Elabd, Y. A. *J. Polym. Sci. Part A: Polym. Phys.* **2012**, *50*, 552–562.
- 17 Arges, C.; Jung, M.; Johnson, G.; Parrondo, J.; Ramani, V. *ECS Trans.* **2011**, *41*, 1795–1816.
- 18 Chempath, S.; Boncella, J. M.; Pratt, L. R.; Henson, N.; Pivovar, B. S. *J. Phys. Chem. C* **2010**, *114*, 11977–11983.
- 19 Edson, J. B.; Macomber, C. S.; Pivovar, B. S.; Boncella, J. M. *J. Membr. Sci.* **2012**, *399–400*, 49–59.
- 20 Matsui, K.; Kikuchi, Y.; Hiyama, T.; Kondo, K.; Akimoto, A.; Seita, T.; Watanabe, H. *Fluorocarbon Anion Exchangers and Processes for their Preparation* **1987**.
- 21 Stejskal, E. O.; Tanner, J. E. *J. Chem. Phys.* **1965**, *42*, 288.
- 22 Stallmach, F.; Galvosas, P. *Annu. Rep. NMR Spectrosc.* **2007**, *61*, 51–131.
- 23 Perusich, S. A. *J. Appl. Polym. Sci.* **2010**, *120*, 165–183.
- 24 Swaminathan, P.; Disley, P. F.; Assender, H. E. *J. Membr. Sci.* **2004**, *234*, 131–137.
- 25 Danilczuk, M.; Lin, L.; Schlick, S.; Hamrock, S. J.; Schaberg, M. S. *J. Power Sources* **2011**, *196*, 8216–8224.
- 26 Kim, Y. S.; Kim, D.-S.; Labouriau, A.; Fujimoto, C.; Hibbs, M.; Hays, C. C.; Narayan, S. FY 2010 Annual Progress Report, DOE Hydrogen Program; Arlington, VA, **2010**; pp 967–970.
- 27 Halseid, R.; Vie, P. J. S.; Tunold, R. *J. Electrochem. Soc.* **2004**, *151*, A381.
- 28 Slade, R. C. T.; Varcoe, J. R. *Solid State Ionics* **2005**, *176*, 585–597.
- 29 Fujimura, M.; Hashimoto, T.; Kawai, H. *Macromolecules* **1981**, *14*, 1309–1315.
- 30 Gebel, G.; Lambard, J. *Macromolecules* **1997**, *30*, 7914–7920.
- 31 Simpson, J.; Carr, H. *Phys. Rev.* **1958**, *111*, 1201–1202.
- 32 Klaus, Z. In *Diffusion*, 3rd ed; Niles, S., Ed.; Bruker: Rheinstetten, Germany, **2009**; pp 1–138.
- 33 Zhao, Q.; Majsztrik, P.; Benziger, J. *J. Phys. Chem. B* **2011**, *115*, 2717–2727.
- 34 Kidena, K.; Ohkubo, T.; Takimoto, N.; Ohira, A. *Eur. Polym. J.* **2010**, *46*, 450–455.
- 35 Park, J. K.; Li, J.; Divoux, G. M.; Madsen, L. A.; Moore, R. B. *Macromolecules* **2011**, *44*, 5701–5710.
- 36 Tsushima, S.; Teranishi, K.; Hirai, S. *Energy* **2005**, *30*, 235–245.
- 37 Gebel, G.; Aldebert, P.; Pineri, M. *Macromolecules* **1987**, *20*, 1425–1430.
- 38 Aieta, N. V.; Stanis, R. J.; Horan, J. L.; Yandrasits, M. A.; Cookson, D. J.; Ingham, B.; Toney, M. F.; Hamrock, S. J.; Her-ring, A. M. *Macromolecules* **2009**, *42*, 5774–5780.
- 39 Saccà, A.; Carbone, A.; Pedicini, R.; Portale, G.; D'Ilario, L.; Longo, A.; Martorana, A.; Passalacqua, E. *J. Membr. Sci.* **2006**, *278*, 105–113.